Available online at www.sciencedirect.com
SCIENCE DIRECT
Journal of Catalysis 233 (2005) 442–452
JOURNAL OF CATALYSIS
www.elsevier.com/locate/jcat

Transient studies on the mechanism of N_2O activation and reaction with CO and C_3H_8 over Fe-silicalite

Javier Pérez-Ramírez [a,*], Evgenii V. Kondratenko [b], M. Naoufal Debbagh [c,1]

[a] *Laboratory for Heterogeneous Catalysis, Catalan Institution for Research and Advanced Studies (ICREA) and Institute of Chemical Research of Catalonia (ICIQ), Av. Països Catalans 16, E-43007, Tarragona, Spain*
[b] *Institute for Applied Chemistry Berlin-Adlershof, Richard-Willstätter-Str. 12, D-12489 Berlin, Germany*
[c] *Department of Inorganic Chemistry, University of Alicante, P.O. Box 99, E-03080 Alicante, Spain*

Received 16 January 2005; revised 15 May 2005; accepted 20 May 2005

Available online 16 June 2005

Abstract

The mechanism of the reaction of N_2O and ^{13}CO over Fe-silicalite was investigated with the use of the temporal analysis of products (TAP) reactor and compared with that of the reaction of N_2O and C_3H_8 previously reported (Appl. Catal. A 267 (2004) 181). Upon direct N_2O decomposition at 523–573 K, Fe-silicalite stored ca. 10^{18} atoms of oxygen per gram, with a ratio of 1 O atom per each 30–60 Fe atoms in the sample. Only a small fraction of the deposited oxygen was reactive for CO oxidation. Pump-probe experiments at different time delays (0–2 s) between the pulses of nitrous oxide and the reducing agent indicated the markedly different mechanisms of the N_2O–^{13}CO and N_2O–C_3H_8 reactions in the temperature range of 623–673 K. Fe-silicalite is active for propane oxidation in the presence of short-lived oxygen species, that are produced when N_2O and C_3H_8 are pulsed simultaneously. Time delays between the N_2O and C_3H_8 pulses greater than 0.1 s are sufficient to transform these active oxygen species for hydrocarbon conversion into inactive ones. In contrast, the oxidation of CO by N_2O does not depend on the lifetime of the oxygen species in the range of time delays investigated. The mechanisms of the N_2O-mediated ^{13}CO and C_3H_8 oxidations differ as a consequence of the different interactions of the two reducing agents with iron species in the zeolite. Pulse experiments support the occurrence of the scavenging mechanism with both propane and carbon monoxide. In this mechanism, short-lived oxygen deposited by N_2O is efficiently eliminated by the reductant. Distinctive to propane, the strikingly high affinity of carbon monoxide for isolated Fe^{3+} ions in the zeolite gives rise to an additional pathway for N_2O reduction in the presence of chemisorbed CO species. These particular Fe^{3+}–CO species were identified by in situ UV/vis and EPR spectroscopies (J. Catal. 223 (2004) 13).

Keywords: N_2O decomposition; N_2O reduction; Fe-silicalite; Iron zeolites; Oxygen species; CO; C_3H_8; Mechanism; TAP reactor

1. Introduction

Fe-MFI zeolites are attractive catalysts for N_2O abatement in tail gases from chemical production and stationary combustion processes, where N_2O coexists with other components such as O_2, NO_x, H_2O, and SO_2 [1,2]. In these sources, the temperature determines the type of catalytic after-treatment [3,4]. Iron zeolites show insufficient activities for direct N_2O decomposition in tail gases at temperatures lower than 675 K, because of the slow desorption of oxygen and the inhibiting effect of water vapor [4]. The presence of reducing agents accelerates the removal of oxygen species deposited by N_2O from the catalyst surface by selective catalytic reduction (SCR), resulting in a decreased operation temperature. Light hydrocarbons (C_1–C_3) have been mostly applied for SCR of N_2O over iron zeolites [4–12]. Delahay et al. [13] compared the influence of the reducing agent (H_2, NH_3, CO, C_3H_6, and n-$C_{10}H_{22}$) on the performance of ion-exchanged Fe-beta zeolite for SCR of N_2O in the presence of excess O_2. CO was found to be the most effective selective reductant in the low-temperature range,

* Corresponding author. Fax: +34-977-920-224.
E-mail address: jperez@iciq.es (J. Pérez-Ramírez).
[1] On leave from Département de Chimie, Université Abdelmalek Essaâdi, Tétouan, Morocco.

0021-9517/$ – see front matter
doi:10.1016/j.jcat.2005.05.014

leading to significant N_2O conversion at 470 K. A more recent study by Nobukawa et al. [12] has concluded that CH_4 gives a higher N_2O conversion than CO and H_2 over Fe-MFI catalysts in the absence of O_2.

The considerable number of works reporting catalytic data for iron zeolites in SCR of N_2O contrasts with a few publications assessing the intrinsic reaction mechanism of the process. Exceptionally, the reaction of N_2O and CH_4 over Fe-beta has been investigated in detail by the group of Kunimori, who used in situ infrared spectroscopy, temperature-programmed desorption, and pulse techniques [14–16]. These studies concluded that short-lived oxygen species (denoted hereafter as O*), present on the catalyst surface when N_2O and CH_4 are fed together, efficiently activate methane at low temperature (>473 K). This leads to reactive methoxide species (Fe–OCH_3), which are further oxidized by N_2O, with the possible formation of intermediate formate species (Fe–OOCH), finally leading to N_2, CO_2, and H_2O, and the regeneration of the active iron site (Fe–OH). In contrast, the reaction of CH_4 with the N_2O-pretreated catalyst yielded very low activities even at 623 K. Based on earlier work by Au and Roberts [17] with the $NH_3 + N_2O$ reaction on a Mg(0001) surface, Kunimori et al. [14–16] have distinguished two types of oxygen species derived from N_2O activation: (highly reactive) nascent oxygen transient species (O*) and (nonreactive) thermally accommodated oxygen species (O). In good agreement, the different reactivity of oxygen species from N_2O, depending on their lifetime, was also concluded from our recent study of the $N_2O + C_3H_8$ reaction over steam-activated Fe-MFI catalysts in the temporal analysis of products (TAP) reactor [18]. Accordingly, several pieces of evidence concur on the assumption that short-lived oxygen species formed upon N_2O decomposition [Eq. (1)] are responsible for the hydrocarbon activation and subsequent conversion [Eq. (2)].

$$N_2O + * \rightarrow N_2 + O^* \quad (1)$$

$$HC + O^* \rightarrow CO_2 + H_2O + * \quad (2)$$

$$CO + O^* \rightarrow CO_2 + * \quad (3)$$

$$CO + * \rightarrow CO^* \quad (4)$$

$$N_2O + CO^* \rightarrow CO_2 + N_2 + * \quad (5)$$

For the $N_2O + CO$ reaction over FeZSM-5, it has been also proposed that CO scavenges adsorbed atomic oxygen species deposited by N_2O, leading to N_2 and CO_2 [Eqs. (1) and (3)] [19]. Panov et al. [20,21] determined that α-oxygen, formed by decomposition of N_2O at temperatures less than 573 K over certain Fe^{2+} sites in iron-containing zeolites, reacts with CO in a stoichiometric ratio of 1:1. However, Kiwi-Minsker et al. [22] observed that only a fraction of the oxygen atoms stored on an iron-containing H-ZSM-5 upon N_2O decomposition participates in CO oxidation. This result indicates a parallel between carbon monoxide and light hydrocarbons as N_2O reductants, strongly connoting the coexistence of various forms of adsorbed oxygen with distinct reactivity, rather than a single type of species.

A recent study using in situ UV/vis and EPR spectroscopies [23] has demonstrated that the N_2O reduction by CO over differently prepared FeMFI zeolites is more complex than originally outlined. This involved not only the classic scavenging mechanism in Eqs. (1) and (3) occurring over oligonuclear iron clusters via a redox Fe^{3+}/Fe^{2+} process, but also the reduction of N_2O with coordinated CO species over isolated Fe^{3+} ions [Eqs. (4) and (5)]. Steam-activated Fe-silicalite, containing mostly isolated iron ions in extraframework positions, showed the highest activity per mole of iron [23]. Based on this, it was proposed that the pathways in Eqs. (4) and (5) contribute significantly to the overall reaction rate. Gaining further insight into the mechanism of the $N_2O + CO$ reaction on this particular catalyst is of fundamental and practical interest, especially if a detailed understanding of the differences between the interactions of carbon monoxide and light hydrocarbons with nitrous oxide could be achieved.

In this work, we have applied a transient pulse technique, the TAP reactor, with isotopic tracers in order to quantitatively investigate the process of N_2O activation over steam-activated Fe-silicalite and the interaction of the generated oxygen species with ^{13}CO. The mechanism of the $N_2O + {}^{13}CO$ reaction has been comparatively discussed with that of the $N_2O + C_3H_8$ reaction analyzed previously [18]. The mechanistic aspects elucidated here are relevant for deriving rational microkinetic models to predict steady-state catalytic performances for N_2O abatement over iron-containing zeolites, a process of prominent importance in environmental catalysis.

2. Experimental

2.1. Catalyst

Details of the hydrothermal synthesis of isomorphously substituted Fe-silicalite have been described elsewhere [24]. The as-synthesized sample was calcined in air at 823 K for 10 h and converted into the H-form by three consecutive exchanges with a NH_4NO_3 solution (0.1 M) for 12 h and subsequent air calcination at 823 K for 5 h. Finally the catalyst was activated in a flow of nitrogen and steam at 1 bar, with the use of a partial steam pressure of 300 mbar and 30 ml STP N_2 min^{-1} at 873 K for 5 h. Characterization studies of the steam-activated Fe-silicalite ($Si/Al \approx \infty$ and 0.68 wt% Fe) indicated a rather uniform distribution of iron species dominated by isolated iron ions in extraframework positions. A certain fraction of oligonuclear iron-oxo species in the zeolite channels was also identified, but clustering into large iron oxide particles was totally prevented [23,24].

2.2. Transient studies

Transient experiments were performed in the TAP reactor, a pulse technique with a time resolution in the sub-

millisecond range. The TAP-2 reactor system has been described in detail elsewhere [25,26]. The catalyst (50 mg, 250–355 μm) was packed between two layers of quartz spheres of the same size fraction in the quartz reactor (6 mm id). Before the experiments, Fe-silicalite was pretreated in flowing He (30 ml STP min^{-1}) at 773 K and atmospheric pressure for 2 h. The pretreated sample was then exposed to vacuum (10^{-5} Pa), and pulse experiments were subsequently performed. Pulse sizes in the range of 10^{14}–10^{15} molecules were dosed by means of high-speed pulse valves. This pulse size range corresponded to the Knudsen diffusion regime, where the interaction of molecules in the gas phase is minimized. Accordingly, purely heterogeneous reaction steps were accounted for. Various types of transient experiments were conducted:

- The concentration of oxygen atoms adsorbed on the zeolite by N_2O decomposition was determined from multipulse experiments. In these, a mixture of $N_2O/Ne = 1/1$ was repetitively pulsed over the He-pretreated catalyst at 523 and 573 K until no N_2O conversion was observed. Approximately 1 min after the last N_2O pulse, multipulse experiments with a mixture of $^{13}CO/Ne = 1/1$ were carried out at the same temperatures in order to probe the deposited oxygen species via CO oxidation to CO_2.
- Direct N_2O decomposition was studied at 673–773 K by single pulsing of a gas mixture of $N_2O/Ne = 1/1$ over the He-pretreated catalyst.
- The reaction of N_2O and ^{13}CO (or C_3H_8) was investigated at 623 and 673 K by means of pump-probe experiments. Mixtures of $N_2O/Xe = 1/1$ and $^{13}CO/Ne = 1/1$ (or $C_3H_8/Ne = 1/1$) were sequentially pulsed in the reactor, with time delays (Δt) between the two mixtures in the range of 0–2 s. Experiments at $\Delta t = 0$ s involved simultaneous pulsing of both mixtures.

The reactants Ne (4.5), Xe (4.0), N_2O (2.0), CO (4.7), ^{13}CO (99 at% ^{13}C, Aldrich), and C_3H_8 (3.5) were used without additional purification. A quadrupole mass spectrometer (Hiden Analytical) was used for quantitative analysis of reactants and reaction products. The transient responses at the reactor outlet were monitored at the following atomic mass units (AMUs): 132 (Xe), 45 ($^{13}CO_2$), 44 (N_2O, CO_2, C_3H_8), 42 (C_3H_6, C_3H_8), 32 (O_2), 30 (N_2O), 29 (C_3H_8, ^{13}CO), 28 (N_2, CO, N_2O, CO_2, C_3H_8, C_3H_6), 20 (Ne), and 18 (H_2O). The individual AMUs in multi-pulse experiments were recorded without averaging. In other experiments, 10 pulses were recorded and averaged for each AMU in order to improve the signal-to-noise ratio. This was done once stable transient responses of the chemical species involved were obtained. The variations in feed components and reaction products were determined from the respective AMUs with the use of standard fragmentation patterns and sensitivity factors.

3. Results and discussion

3.1. Direct N_2O decomposition versus N_2O reduction

In order to understand primary mechanistic differences between direct N_2O decomposition and N_2O reduction, single pulsing of N_2O and simultaneous pulsing of N_2O–^{13}CO and N_2O–C_3H_8 were conducted in the TAP reactor at different temperatures (Fig. 1). The transient responses in this figure were normalized for a better comparison of pulse shapes, which provide valuable qualitative information about the reaction mechanisms. During direct N_2O decomposition at 773 K (Fig. 1a), the response of N_2 directly follows that of N_2O, whereas the response of O_2 is broader and considerably shifted to longer times. This indicates that N_2 formation is faster than O_2 formation, in conformity with the well-accepted fact that the overall reaction rate of direct N_2O decomposition is limited by oxygen desorption from the catalyst surface [12,27–29]. The uncoupling of the N_2 and O_2 signals in Fig. 1a indicates that in this temperature range, O_2 should be formed mainly by the slow recombination and desorption of surface oxygen atoms according to Eq. (6), regenerating the active site. A recent work has correlated the shape of the oxygen response during single pulsing of N_2O in the TAP reactor with the steady-state performance of steam-activated FeMFI zeolites in direct N_2O decomposition [30]. The sharper the O_2 signal, the higher the N_2O conversion due to an improved oxygen desorption, which is essentially determined by the forms of iron species in the catalyst.

$$O^* + O^* \rightarrow O_2 + 2^* \quad (6)$$

Active site regeneration can be strongly accelerated by the addition of reducing agents, leading to a reduced operation temperature for N_2O abatement by facilitated O^* removal [Eqs. (2) and (3)] [4]. As a matter of fact, the N_2O conversion in the presence of CO or C_3H_8 (Figs. 1b–c) was 90 and 83% at 673 K, respectively, as compared with the N_2O conversion of 70% at 773 K in direct decomposition (Fig. 1a). The effect of CO and C_3H_8 can be mechanistically explained, with attention to the shape of the transient responses in Fig. 1. For example, the reaction products of N_2O reduction and ^{13}CO oxidation, N_2 and $^{13}CO_2$, appear at very similar times (Fig. 1b), contrasting with the delay of the O_2 response with respect to that of N_2 in direct N_2O decomposition. Accordingly, the removal of O^* species by CO, yielding CO_2, is much faster than the recombination of O^* species in direct N_2O decomposition. In this study, isotopically labeled ^{13}CO and nonlabeled $^{14}N_2O$ were used to uncouple the analysis of N_2O–CO_2 and CO–N_2 in mass spectrometry. The use of the most abundant isotopes for dinitrogen oxide and carbon monoxide makes it impossible to discriminate between them because of the identical main masses of $^{14}N_2O$ and $^{12}CO_2$ (AMU 44) and of $^{14}N_2$ and ^{12}CO (AMU 28). In a manner very similar to that of the

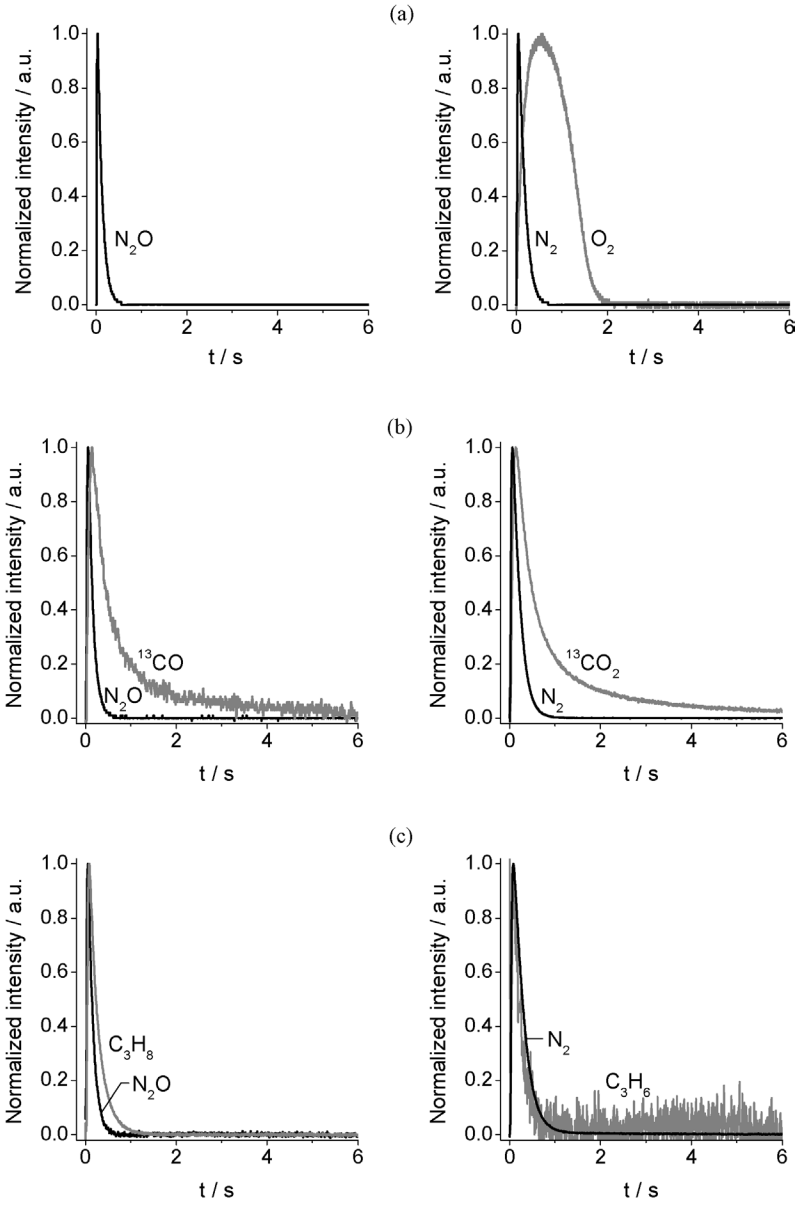

Fig. 1. Transient responses of reactants and products during (a) single pulsing of N_2O at 773 K, (b) simultaneous pulsing of N_2O and ^{13}CO at 673 K, and (c) simultaneous pulsing of N_2O and C_3H_8 at 673 K over Fe-silicalite. Pulse size of N_2O, CO, and $C_3H_8 \approx 2 \times 10^{14}$ molecules.

N_2O–^{13}CO system, the responses of the N_2 and C_3H_6 products upon simultaneous pulsing of N_2O–C_3H_8 at 623 K are also nicely coupled (Fig. 1c). It should be pointed out that propylene is a primary product of the oxidative dehydrogenation of propane with N_2O, where steam-activated iron zeolites have demonstrated superior performance [18,31,32]. CO_2 was also formed in the reaction as a product of the total propane oxidation (cf. Section 3.4). This would be the main C-product of the reaction when O_2 is in the feed, as shown in steady-state studies dealing with the C_3H_8-SCR of N_2O in the presence of excess oxygen [6,7].

The type of pulse experiments presented in Figs. 1b–c further confirms that both CO and C_3H_8 are efficient O^* scavengers according to Eqs. (2) and (3) but does not demonstrate conclusive differences between the modus operandi of the two reactants for N_2O reduction. It is worth noting in particular the pronounced tailing of the ^{13}CO and $^{13}CO_2$ responses over Fe-silicalite (up to 6 s) as compared with those of C_3H_8 and C_3H_6 (ca. 1 s). This indicates a strong interaction of carbon monoxide with the catalyst, accompanied by a very slow desorption process. As elaborated in Section 3.4, this aspect turns out to be of paramount importance to the elucidation of the principal mechanistic differences between CO and C_3H_8 in the catalytic reduction of N_2O over Fe-silicalite.

3.2. Active sites for N_2O activation

The O_2/N_2 ratio at the reactor outlet during the single N_2O pulse experiment in Fig. 1a was ca. 1:3, indicating a

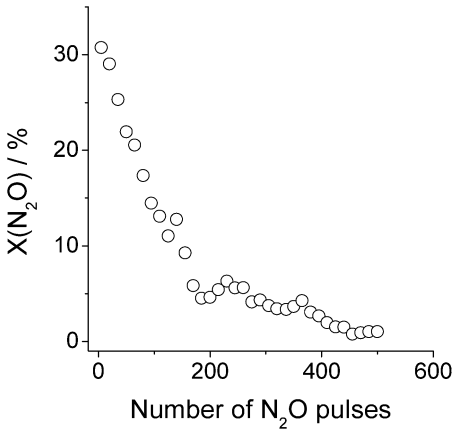

Fig. 2. N_2O conversion over Fe-silicalite in multi-pulse experiments at 573 K. Pulse size of $N_2O \approx 3 \times 10^{15}$ molecules.

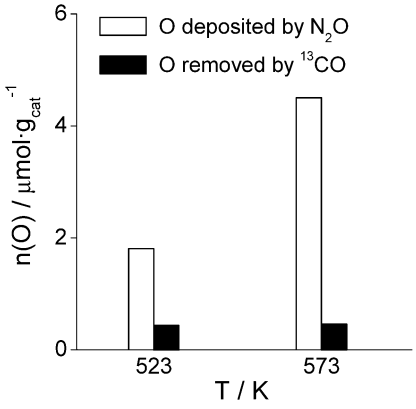

Fig. 3. Amount of atomic oxygen irreversible adsorbed on Fe-silicalite upon direct N_2O decomposition and amount of atomic oxygen removed by probing the resulting oxidized surface by ^{13}CO at different temperatures.

certain consumption of oxygen by the zeolite. Indeed, no O_2 was produced over the iron-containing zeolite at $T < 673$ K; N_2 was the only decomposition product detected. Taking into account this experimental observation, we carried out multi-pulse experiments with N_2O in the TAP reactor over Fe-silicalite (pretreated in He at 723 K) in order to determine the capacity of the sample to store oxygen species at 523 and 573 K. This should provide a measure of the number of sites for N_2O decomposition according to Eq. (1). Following the original nomenclature by Panov, these sites are referred to in the literature as α-sites and have been defined as Fe^{2+} species in the zeolite, which are reversibly oxidized to Fe^{3+} species by N_2O, generating α-oxygen [20,33]. This form of active surface oxygen readily exchanges with O_2 and oxidizes CO and CH_4 already at room temperature, and benzene to phenol at moderate temperatures [34].

A typical curve resulting from the multi-pulse experiments with N_2O at 573 K is shown in Fig. 2. It should be noted that the peak N_2O pressure in these experiments at the pulse size applied (3×10^{15} molecules) is ca. 0.2 Torr and that the number of N_2O molecules in one pulse is 10^3 times smaller than the total number of iron atoms in the catalyst. The N_2O conversion in the first pulse (ca. 30%) decreases with the pulse number as a consequence of the gradual saturation of the active sites in the catalyst. The decrease is sharper during the first 200 pulses and gradually approaches the value of zero conversion after 500 pulses. The amount of atomic oxygen deposited in the zeolite upon N_2O activation is shown as empty bars in Fig. 3, increasing from 1.8 µmol O g_{cat}^{-1} at 523 K to 4.5 µmol O g_{cat}^{-1} at 573 K. These values can be expressed as a concentration of sites, assuming that a single oxygen atom is chemisorbed on each active site, resulting in 1.1×10^{18} and 2.7×10^{18} sites g_{cat}^{-1} at 523 and 573 K, respectively. Similarly, Kiwi-Minsker et al. [22] determined concentrations of sites (referred to as C_{ad}) in the range of 10^{17}–10^{18} sites g_{cat}^{-1} with a transient step-change method at a partial N_2O pressure of 15 Torr over H-ZSM-5 with iron contents in the range of 70–1000 ppm and experienced a slight increase in C_{ad} upon increasing the reaction temperature from 523 to 603 K. Higher concentrations of α-sites, on the order of 10^{19} sites g_{cat}^{-1}, have been determined by Dubkov et al. [35,36] over FeZSM-5 with 0.8 wt% Fe_2O_3; they used their well-established static method at low partial N_2O pressures (0.2–0.4 Torr) at 523 K and isotopic oxygen exchange at 323 K. The different nature of the experimental techniques applied may explain the discrepancies in the determined concentration of active sites for N_2O decomposition. However, the dissimilar genesis of the zeolite catalysts in the various studies with respect to the iron content, synthesis method, and activation procedure, which strongly influence the forms of iron in the final material, will also affect the obtained concentrations of active sites for the reaction. For example, it has recently been reported that the ratio between the amount of oxygen deposited by N_2O decomposition at 473 K and the iron content (O_{dep}/Fe) in Fe-ferrierite zeolites with Fe/Al = 0.05–0.25 increased from 0.5 to 1 as the sample pretreatment temperature was increased from 723 to 973 K [37].

In our case, the amount of atomic oxygen deposited on the catalyst as determined from the multi-pulse experiments represents only 1.5% (at 523 K) and 3.7% (at 573 K) of the total iron content in Fe-silicalite (122 µmol Fe g_{cat}^{-1}). This indicates that a very large fraction of the iron in the zeolite (>95%) is unable to activate the N_2O molecule under TAP conditions at these temperatures.

3.3. Titration of adsorbed oxygen species with ^{13}CO

Approximately 1 min after saturation of Fe-silicalite by atomic oxygen species resulting from N_2O decomposition, multi-pulses of ^{13}CO were introduced at the same temperature. The aim of this experiment was to probe the oxygen species [deposited by N_2O, Eq. (1)] that are active for CO oxidation, according to Eq. (3). The results obtained were surprising, since the amount of oxygen reacting with ^{13}CO was 4 and 10 times lower than the amount of oxygen deposited by N_2O and was not temperature dependent (solid bars in Fig. 3). Since no O_2 desorption was observed in the period of time between the last N_2O pulse in Fig. 2 and the

first ^{13}CO pulse in the titration experiments, a large fraction of oxygen species deposited over Fe-silicalite during N_2O decomposition was concluded to be irreversibly adsorbed in the zeolite and unable to oxidize CO. Our results are in line with a recent work by Kiwi-Minsker et al. [22], who investigated the oxidation of CO at 523 K over iron-doped H-ZSM-5, which was pre-covered by oxygen species (O_{ad}) resulting from N_2O decomposition at the same temperature. These authors concluded that the amount of O_{ad} consumed (or CO_2 formed) corresponds to ca. 65% of the total amount of atomic oxygen chemisorbed from N_2O, whereas in our case the percentages of oxygen species reacted with CO amount to 24% at 523 K and 10% at 573 K of the total oxygen species deposited by N_2O. To explain the reactivity of a fraction of adsorbed oxygen species for CO oxidation, Kiwi-Minsker et al. [22] proposed the presence of two oxygen pools: one with the oxygen capable of reacting with CO and the other with adsorbed oxygen, which was not active. These results are in contradiction to those reported by the group of Panov [20,21], establishing that the stoichiometry of the reaction between α-oxygen and carbon monoxide over Fe-containing ZSM-5 zeolite is 1:1, leading to CO_2 in amounts equal to those of α-oxygen on the surface. It should be noted that in contrast to our experiments, Panov et al. determined the $CO{:}O_\alpha$ stoichiometry from the reaction between O_α (deposited by N_2O decomposition at 523 K) and CO at 373 K.

The hypothesis of two oxygen pools in the $N_2O + CO$ reaction [22] fits nicely with the mechanistic description of the $N_2O + C_3H_8$ reaction [18] and the $N_2O + CH_4$ reaction [14–16]. In the latter, Kunimori et al. discerned two types of adsorbed oxygen species on Fe-beta: "nascent oxygen transient" able to activate CH_4 at 473 K and "thermally accommodated oxygen" that is hardly able to activate CH_4 even at 623 K. These studies are further discussed in Section 3.4 in relation to our sequential pulse experiments between N_2O and C_3H_8. The "oxygen pools" concept was also proposed by Pirngruber [28] to account for the two different O_2 desorption processes during direct N_2O decomposition over Fe-zeolites prepared by sublimation: one oxygen pool desorbed relatively fast from a small fraction of sites (responsible for catalytic activity), and a second oxygen pool desorbed very slowly from the catalyst.

Related studies in agreement with the observations here and in [14–16,22,28] have been also reported by Jia et al. [38]. These authors investigated the exchange of $^{18}O_2$ at 523 K with a Fe/MFI prepared by chemical vapor deposition, which was previously treated in N_2 ^{16}O at the same temperature. The experiments unequivocally concluded that the number of exchangeable oxygen atoms was smaller than the number of oxygen atoms deposited by N_2O. Using Fe-ferrierite zeolites with $Fe/Al = 0.03$–0.6, Nováková et al. [39] also concluded that the amount of oxygen participating in ^{18}O isotopic exchange at room temperature is 30–50% lower than the amount of oxygen captured by the catalysts upon N_2O decomposition at 473 K. The results in [38,39] agree well with earlier work by Leglise et al. [40] on the limited redox capacity of ion-exchanged iron mordenite for oxygen isotopic exchange during N_2 ^{16}O decomposition experiments over ^{18}O-treated catalysts, which did not conform to the authors' expectations.

The results derived from our multi-pulse experiments in the TAP reactor and from previous works [14–16,18,22,28,38–40] produce unquestionable evidence that not all of the atomic oxygen deposited by N_2O on active iron sites in the zeolite exhibit the described reactivity properties for α-oxygen [20,21,33–36]. The deposited O atoms include (at least) more than one type of adsorbed oxygen species with low activity for CH_4 oxidation [14–16], C_3H_8 oxidation [18], CO oxidation [22], O_2 desorption during N_2O decomposition [28], and isotopic oxygen exchange [38,39].

3.4. Interaction of O-species from N_2O with reducing agents: ^{13}CO versus C_3H_8

The reaction of adsorbed oxygen species generated upon N_2O decomposition with ^{13}CO and C_3H_8 was investigated at 623 and 673 K by means of pump-probe experiments in the TAP reactor. To this end, N_2O and ^{13}CO (or N_2O and C_3H_8) were sequentially pulsed, with a time delay between them in the range of 0–2 s. The application of short and variable time delays in sequential pulsing represents a unique feature of the TAP reactor, particularly for the analysis of the influence of the lifetime of the oxygen species deposited by N_2O on their reactivity for the oxidation of carbon monoxide or propane.

Fig. 4 shows the conversion of reactants and yield of products during these experiments over Fe-silicalite, which indicate the markedly different performance and reaction mechanism, depending on the reductant applied. At $\Delta t = 0$ s, that is, when N_2O and ^{13}CO (or N_2O and C_3H_8) were simultaneously pulsed, the conversion of ^{13}CO (ca. 80%) was significantly higher than the conversion of C_3H_8 (ca. 50%). Associated with this, the N_2O conversion was also higher with ^{13}CO than with C_3H_8 (e.g., 70% vs. 50% at 623 K). From this result, it can be concluded that N_2O oxidizes carbon monoxide more easily than it does propane, or in other words, that CO is a better reducing agent for the conversion of N_2O to N_2 over our catalyst. Furthermore, another revealing feature originally reported in [18] and shown for comparative purposes in Fig. 4 is the strong decrease in propane conversion that occurs with an increasing time delay between the N_2O and C_3H_8 pulses, approaching zero at $\Delta t = 2$ s. The same behavior was observed in the yield of the main products, C_3H_6 and CO_2. In contrast, pump-probe experiments with N_2O–^{13}CO show that the ^{13}CO conversion and $^{13}CO_2$ yield were not affected by the time delay between the N_2O and ^{13}CO pulses.

The latter result apparently indicates that the reactivity of the oxygen species deposited by N_2O toward ^{13}CO oxidation does not change in the range of 0–2 s. In contrast, the dependencies observed in the N_2O–C_3H_8 system highlight the vital importance of the lifetime of atomic oxygen

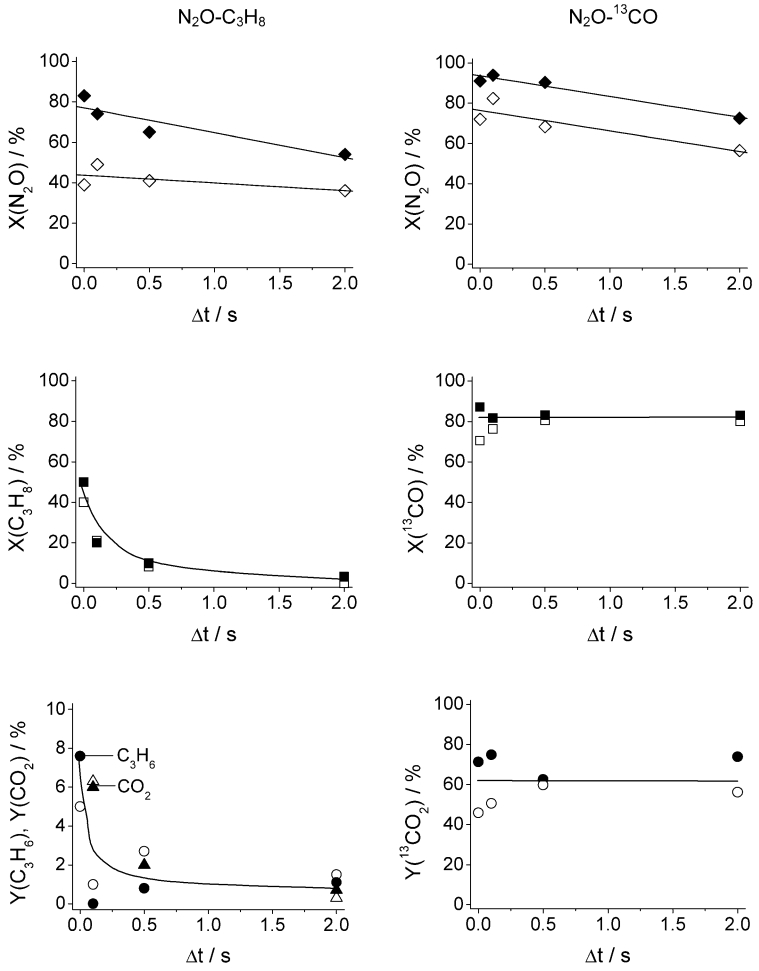

Fig. 4. Conversion of reactants and yield of products vs time delay during sequential pulse experiments of N_2O–C_3H_8 and N_2O–^{13}CO at 623 K (open symbols) and 673 K (solid symbols). Pulse sizes of N_2O, C_3H_8, and ^{13}CO were in the range of 2×10^{14}–5×10^{14} molecules.

species deposited by nitrous oxide for propane conversion: short-lived oxygen species at $\Delta t = 0$ s effectively activate propane [Eq. (7)], which cannot be accomplished by long-lived oxygen species at $\Delta t > 0.1$ s. Once again, this result draws a remarkable parallel with previous work on the $N_2O + CH_4$ reaction over Fe-beta, where "short-lived oxygen" is referred to as "nascent or hot oxygen transients," and "long-lived oxygen" is referred to as "thermally accommodated oxygen." From our experiments, a decrease in the concentration of adsorbed atomic oxygen induced by its desorption can be categorically excluded as a reason for the decreased propane conversion at increased time delays, since no gas-phase O_2 was ever observed. Accordingly, it is reasonable to postulate a rapid transformation of highly reactive species (O^*, active pool) into highly stabilized species ($O\triangle$, inactive pool), according to Eq. (8).

$$C_3H_8 + O^* \rightarrow C_3H_6, CO_2 + H_2O + * \quad (7)$$

$$O^* + \triangle \rightarrow O\triangle + * \quad (8)$$

At this stage, no definitive experimental evidence has been gathered to assess the nature and location of the proposed $O\triangle$ species. Based on pioneering work by the group of Hall, it can be proposed that the number of active O^* species, decreased because of their limited lifetime, may involve their incorporation into vacancies of the zeolite matrix. This implies the dynamic nature of the adsorbed oxygen in the zeolite and the presence of oxygen vacancies in the zeolite. The mobility of oxygen species (in both lattice ions and adsorbed species) was elegantly demonstrated by Valyon et al. [41] with step-switching experiments from N_2 ^{16}O to N_2 ^{18}O over Fe-mordenite. In that work, it was also found that ~ 7 times more ^{18}O could be accommodated than Fe present in the sample. Accordingly, Fe was proposed as a "porthole" through which this ^{18}O was incorporated into the vicinity of the zeolite matrix. Further support for this model comes from works by Nováková et al. [39,42]. In these, the labilization of framework oxygen in Fe-ferrierites was demonstrated by $^{18}O_2$ isotopic exchange followed by TPD experiments over N_2 ^{16}O-pretreated samples, since mostly $^{16}O_2$ was analyzed at the reactor outlet above 473 K.

We have observed that the propane conversion and the corresponding yield of products at $\Delta t = 0.1$ s and 0.5 s, for example, did not change after ca. 200 cycles in sequential

pulse experiments. This result indicates that the amount of active sites for the $N_2O + C_3H_8$ does not decrease, thus suggesting that active sites for C_3H_8 oxidation by O^* are not eventually saturated by the presence of inactive $O\triangle$ species. In agreement with this conclusion, the practically unchanged N_2O conversion with an increased time delay in Fig. 4 suggests a rather constant number of active sites for the generation of highly reactive O^* species from nitrous oxide decomposition. This can be tentatively explained by a certain balance between (i) the removal of O^* by propane [Eq. (7)], which prevails at $\Delta t = 0$ s, and (ii) the transformation of reactive oxygen species into inactive ones [Eq. (8)], which is favored by long time delays. According to this, the slight decrease in N_2O conversion that occurs with an increased time delay is indicative of the faster removal of O^* by the hydrocarbon as compared with the self-diffusion of O^* into vacancies of the zeolite framework.

The transformation in Eq. (8) can also account for the low ratio between the amount of CO_2 produced in the titration studies with CO multi-pulses and the amount of atomic oxygen deposited upon saturation of Fe-silicalite with N_2O (Fig. 3), and in related works assessing the reactivity of adsorbed oxygen with CO [22]. It should be stressed that the time between the last N_2O pulse and the first CO pulse in the multi-pulse experiments described in Sections 3.2 and 3.3 was ca. 1 min. Similarly, Kiwi-Minsker et al. [22] deposited O species on H-ZSM-5 by N_2O pretreatment at 523 K, followed by a 15-min purge with He, and the subsequent admission of CO for 6 min at 523 K. Panov et al. [20,21] investigated the reaction of carbon monoxide with α-oxygen according to a similar procedure: deposition of O_α by N_2O decomposition at 523 K, followed by cooling to 373 K, and subsequent reaction with CO. With this experimental methodology and based on our results and [22], the process in Eq. (8) is expected to take place extensively, and the CO:O_α stoichiometry of 1:1 obtained by Panov et al. cannot be substantiated by our observations.

Several causes can be put forward to explain the remarkably constant conversion of carbon monoxide in sequential N_2O–^{13}CO pulsing experiments in Fig. 4. In contrast to the case of propane, it could be inferred that the adsorbed oxygen species generated from N_2O have the same reactivity for ^{13}CO oxidation in the range of time delays investigated. Based on our previous discussion, this suggests that the eventual transformation of the short-lived oxygen species does not lead to an inactive form of adsorbed oxygen for ^{13}CO oxidation. This is rather unlikely, however, based on the low reactivity of oxygen species deposited by N_2O in the titration experiments with ^{13}CO multi-pulses, even if the 1-min interval between the last N_2O pulse and the first CO pulse largely exceeds the maximum time delay of 2 s in pump-probe experiments. Another explanation for the observed behavior in Fig. 4 with carbon monoxide is that this reactant would catalyze, in an adsorbed form, the reduction of N_2O. CO adsorption in the titration experiment is adverse because of the blockage by oxygen species deposited in the previous step by N_2O decomposition, implying competitive adsorption of CO and N_2O for the same active iron sites. Accordingly, this type of experiment merely examines the elementary step represented by Eq. (2). The number of adsorption sites during pump-probe experiments is 10^3 times higher than the amount of reactants pulsed, so that both O^* and CO^* species derived from N_2O decomposition and CO adsorption, respectively, may coexist. The validity hypothesis has been proved in Section 3.5.

3.5. Mechanism of N_2O reduction in the presence of adsorbed CO species

As expressed in Section 3.1, simultaneous pulsing of N_2O–C_3H_8 and N_2O–^{13}CO provided an indication of the different interactions of the reducing agents with Fe-silicalite. The marked tailing of the transient response of carbon monoxide and carbon dioxide as compared with that of propane (compare Figs. 1b–c) denotes a strong interaction of the former gases with the catalyst, inducing a very slow desorption process of both ^{13}CO and $^{13}CO_2$. This feature may be related to the constant ^{13}CO conversion at different time delays in Fig. 4. In the same manner, the weaker interaction of C_3H_8 with the catalyst (sharper responses, Fig. 1c) could be associated with the fast decay of C_3H_8 conversion as the time delay between the N_2O and C_3H_8 pulses in Fig. 4 is increased.

These suppositions were substantiated by analyzing the transient responses of the various species implicated during the pump-probe experiments. The results in Fig. 5 are illustrative of the different affinities of the two reducing agents for the iron species in Fe-silicalite. In the case of N_2O–C_3H_8 experiments (Fig. 5a), the response of propane returns to the baseline ca. 1 s after being pulsed at $t = 2$ s. In addition, as expected, no C-containing products were identified in the N_2O pulse at $t = 0$ s. In contrast, the transient response of ^{13}CO in N_2O–^{13}CO experiments (Fig. 5b) reaches the baseline ca. 5 s after being pulsed at $t = 1$ s, indicating the strong adsorption and slow desorption of carbon monoxide. This statement is reinforced by the observation of substantial amounts of ^{13}CO desorbing from the catalyst at the time of the N_2O pulse at $t = 0$ s. Blank experiments excluded this signal to be caused by an impurity with AMU 29 in the N_2O-containing mixture. This ^{13}CO stayed on the catalyst surface for at least 5 s (period of time from the ^{13}CO pulse at $t = 1$ s to the next N_2O pulse) under vacuum conditions. This result indicates that N_2O decomposes and deposits oxygen species on the same iron sites where CO was adsorbed, inducing its desorption according to Eq. (9).

$$CO^* + N_2O \rightarrow N_2 + CO + O^* \quad (9)$$

Additional insights into the mechanism of the $N_2O + {}^{13}CO$ reaction can be obtained from an analysis of the CO_2 response in pump-probe experiments at 673 K and its dependence on the pulse size. This is illustrated in Fig. 6 for $\Delta t = 1$ s, using ^{13}CO pulse sizes of 2×10^{14} (black line) and

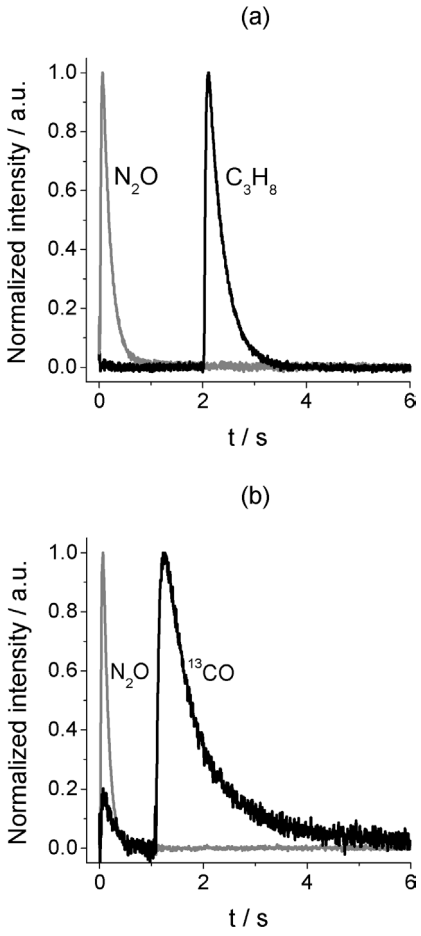

Fig. 5. Transient responses during sequential pulsing of (a) N_2O and C_3H_8 at $\Delta t = 2$ s and (b) N_2O and ^{13}CO at $\Delta t = 1$ s over Fe-silicalite at 673 K. Pulse sizes as in caption of Fig. 4.

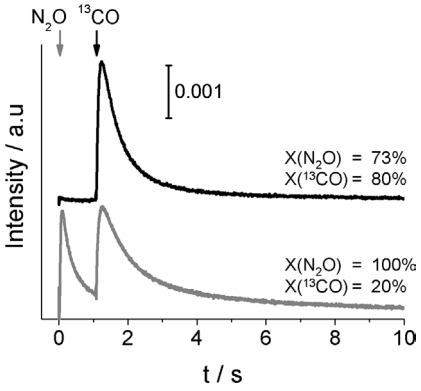

Fig. 6. Influence of the ^{13}CO pulse size on the transient responses of $^{13}CO_2$ and attained degree of ^{13}CO conversion during sequential pulsing of N_2O and ^{13}CO at $\Delta t = 1$ s over Fe-silicalite at 673 K. Pulse size of ^{13}CO was 2×10^{14} molecules (black line) or 1×10^{15} molecules (gray line), keeping constant the pulse size of N_2O at 2×10^{14} molecules.

1×10^{15} (gray line) molecules. The N_2O pulse size was kept constant at 2×10^{14} molecules. At equal pulse sizes of ^{13}CO and N_2O, an intense $^{13}CO_2$ response appeared at the time of the ^{13}CO pulse, and only a minor signal was identified at the time of the N_2O pulse. Furthermore, ^{13}CO and N_2O conversions of 80 and 73% were obtained, respectively. Increasing the pulse size of ^{13}CO by one order of magnitude led to complete N_2O conversion, whereas the ^{13}CO conversion decreased to 20%. This is expected, since the lower amount of N_2O limits the degree of conversion of the reducing agent [23,43]. An important observation from this experiment is the comparable intensity of the transient response of $^{13}CO_2$ in both N_2O and ^{13}CO pulses, which unequivocally indicates two reaction routes for carbon dioxide production, occurring to a similar extent. This feature was never observed in the N_2O–C_3H_8 system; that is, no residual propane or carbon-containing reaction products were observed in the pulse of N_2O, regardless of the pulse size of propane. It should also be pointed out that the $^{13}CO_2$ response at the time of the ^{13}CO pulse presented a more extensive tailing (up to 9 s) when larger pulse sizes of carbon monoxide were applied. This is rather logical, because of the higher surface concentration of C-containing species.

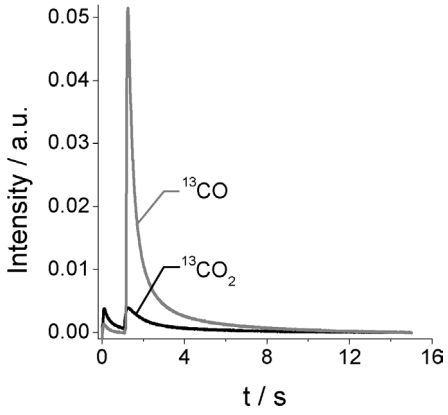

Fig. 7. Transient responses of ^{13}CO and $^{13}CO_2$ during sequential pulsing of N_2O and ^{13}CO with $\Delta t = 1$ s over Fe-silicalite at 673 K. Pulse size of $N_2O = 2 \times 10^{14}$ molecules and pulse size of $^{13}CO \approx 1 \times 10^{15}$ molecules.

In view of the order of the pulses in our sequential N_2O–^{13}CO experiments, it can be proposed that the classic scavenging mechanism proposed in Eqs. (1) and (3) accounts for the $^{13}CO_2$ formed at the time of the ^{13}CO pulse. This pathway principally describes the N_2O reduction by light hydrocarbons like CH_4 [14–16] and C_3H_8 [18]. However, in the case of the $N_2O + CO$ reaction, the previous O^*-assisted CO oxidation is complemented by the N_2O conversion in the presence of adsorbed CO species (denoted as CO^*-assisted N_2O reduction, Eqs. (4) and (5)). The appearance of ^{13}CO and $^{13}CO_2$ as reaction products in the N_2O pulse (cf. Figs. 5b and 7) suggests that strongly adsorbed CO species can undergo two processes in the presence of N_2O: reaction of N_2O with adsorbed CO to yield CO_2 [Eq. (5)] and desorption of CO species by N_2O [Eq. (9)]. As shown in Fig. 7, the relatively higher intensity of the $^{13}CO_2$ signal as compared with the ^{13}CO signal at the time of the N_2O pulse during sequential pulsing at 673 K indicates that Eq. (5) prevails over Eq. (9). It can be tentatively suggested that the step in Eq. (5) alternatively occurs in the presence of adsorbed species [Eq. (10)]. However, assessing a detailed molecular

description of the CO*-assisted N_2O reduction requires further research, since the nature of the exact adsorption site(s) of the participative CO* and O* species is not completely clear at this stage.

$$CO^* + O^* \rightarrow CO_2 + 2^* \quad (10)$$

In any case, we believe that the reduction of N_2O in the presence of adsorbed CO species is responsible for the invariable conversion of ^{13}CO and stable yield of $^{13}CO_2$ at different time delays during sequential N_2O–^{13}CO pulse experiments in Fig. 4. Accordingly, the pathway represented by Eqs. (4) and (5) seems to overcome the transformation of O* species into inactive forms [Eq. (8)] in the Δt range investigated, which is detrimental to the extent of the pathway represented by Eqs. (1)–(3) (as shown in sequential N_2O–C_3H_8 pulse experiments in Section 3.4 and in titration experiments with CO in Section 3.3).

The identification of two reaction pathways in the reaction of N_2O and CO over Fe-silicalite with a transient pulse technique, the temporal analysis of products reactor, agrees well with recent in situ EPR and UV/vis spectroscopic investigations by some of us [23]. These concluded that the above processes are site-dependent: the O*-assisted CO oxidation [Eqs. (1) and (3)] is favored over oligonuclear iron-oxo species and is able to coordinate highly reactive oxygen species by N_2O decomposition [Eq. (1)]. The newly reported CO*-assisted N_2O reduction mainly involved isolated Fe(III) ions in extraframework positions. Steady-state experiments in [23] showed that the highest activity per mole of iron site was obtained for the Fe-silicalite investigated here, which has the highest concentration of such isolated sites among the different materials investigated. Accordingly, the created Fe^{3+}–CO species can be considered to have a very high activity for N_2O reduction. This may be responsible for the high efficiency of CO in the low-temperature catalytic N_2O reduction over iron-containing zeolites.

4. Conclusions

Our TAP studies have elucidated novel mechanistic features of the reaction between N_2O and ^{13}CO or C_3H_8 over Fe-silicalite:

- Multi-pulse experiments concluded that N_2O deposits ca. 10^{18} atoms of oxygen per gram of catalyst upon decomposition at 523–573 K, although subsequent titration showed that a small fraction of the stored oxygen participates in CO oxidation. This suggests the presence of different pools of oxygen species on the catalyst with a markedly distinct oxidizing power.
- In line with this, pump-probe experiments at 623–673 K showed that Fe-silicalite effectively activates propane when N_2O and C_3H_8 are pulsed together. However, these oxygen species become inactive for propane oxidation if the pulses are separated by more than 0.1 s. This agrees with our previous findings and observations by other authors for the reaction between N_2O and CH_4, suggesting a certain regularity of the activation of light hydrocarbons by short-lived oxygen species from N_2O, which rapidly transform and lose their unique reactive character. In contrast to the N_2O–C_3H_8 system, the lifetime of the adsorbed oxygen species did not influence the activation of ^{13}CO over Fe-silicalite in the range of time delays investigated (0–2 s).
- Both the N_2O-mediated ^{13}CO and C_3H_8 oxidations proceed via the classic scavenging mechanism, where the reducing agent is activated by short-lived oxygen species deposited by N_2O on oligonuclear iron species in the zeolite. Furthermore, the reaction of nitrous oxide with carbon monoxide incorporates an additional pathway for CO_2 production, involving the reaction of N_2O with chemisorbed CO species. This CO-mediated N_2O reduction occurs in view of the strong interaction of CO on isolated Fe(III) ions in extraframework positions of the zeolite, as supported by previous in situ UV/vis and EPR spectroscopic studies. This unique feature of CO may account for the remarkably high efficiency of CO for the low-temperature SCR of N_2O.

Acknowledgments

M.N.D. thanks AECI for a fellowship to complete his doctoral studies.

References

[1] J. Pérez-Ramírez, F. Kapteijn, G. Mul, J.A. Moulijn, Chem. Commun. (2001) 693.
[2] J. Pérez-Ramírez, F. Kapteijn, G. Mul, J.A. Moulijn, Appl. Catal. B 35 (2002) 227.
[3] J. Pérez-Ramírez, F. Kapteijn, G. Mul, X. Xu, J.A. Moulijn, Catal. Today 76 (2002) 55.
[4] J. Pérez-Ramírez, F. Kapteijn, K. Schöffel, J.A. Moulijn, Appl. Catal. B 44 (2003) 117.
[5] R.W. van den Brink, S. Booneveld, J.R. Pels, D.F. Bakker, M.J.F.M. Verhaak, Appl. Catal. B 32 (2001) 73.
[6] G. Centi, F. Vazzana, Catal. Today 53 (1999) 683.
[7] J. Pérez-Ramírez, F. Kapteijn, Appl. Catal. B 47 (2004) 177.
[8] K. Yamada, S. Kondo, K. Segawa, Micropor. Mesopor. Mater. 35–36 (2000) 227.
[9] T. Chaki, M. Arai, T. Ebina, M. Shimokawabe, J. Catal. 218 (2003) 220.
[10] S. Kameoka, K. Kita, T. Takeda, S. Tanaka, S. Ito, K. Yuzaki, T. Miyadera, K. Kunimori, Catal. Lett. 69 (2000) 169.
[11] M. Yoshida, T. Nobukawa, S. Ito, K. Tomishige, K. Kunimori, J. Catal. 223 (2004) 454.
[12] T. Nobukawa, M. Yoshida, K. Okumura, K. Tomishige, K. Kunimori, J. Catal. 229 (2005) 374.
[13] G. Delahay, M. Mauvezin, A. Guzmán-Vargas, B. Coq, Catal. Commun. 3 (2002) 385.
[14] S. Kameoka, T. Nobukawa, S. Tanaka, S. Ito, K. Tomishige, K. Kunimori, Phys. Chem. Chem. Phys. 5 (2003) 3328.
[15] T. Nobukawa, M. Yoshida, S. Kameoka, S. Ito, K. Tomishige, K. Kunimori, J. Phys. Chem. B 108 (2004) 4071.

[16] T. Nobukawa, M. Yoshida, S. Kameoka, S. Ito, K. Tomishige, K. Kunimori, Catal. Today 93–95 (2004) 791.
[17] C.T. Au, M.W. Roberts, Nature 319 (1986) 206.
[18] E.V. Kondratenko, J. Pérez-Ramírez, Appl. Catal. A 267 (2004) 181.
[19] F. Kapteijn, G. Mul, G. Marbán, J. Rodríguez-Mirasol, J.A. Moulijn, Stud. Surf. Sci. Catal. 101 (1996) 641.
[20] G.I. Panov, V.I. Sobolev, A.S. Kharitonov, J. Mol. Catal. A. Chem. 61 (1990) 85.
[21] K.A. Dubkov, E.A. Paukshtis, G.I. Panov, Kinet. Catal. 42 (2001) 230.
[22] L. Kiwi-Minsker, D.A. Bulushev, A. Renken, J. Catal. 219 (2003) 273.
[23] J. Pérez-Ramírez, M. Santosh Kumar, A. Brückner, J. Catal. 223 (2004) 13.
[24] J. Pérez-Ramírez, F. Kapteijn, J.C. Groen, A. Doménech, G. Mul, J.A. Moulijn, J. Catal. 214 (2003) 33.
[25] J.T. Gleaves, J.R. Ebner, T.C. Kuechler, Catal. Rev.-Sci. Eng. 30 (1988) 49.
[26] J.T. Gleaves, G.S. Yablonsky, P. Phanawadee, Y. Schuurman, Appl. Catal. A 160 (1997) 55.
[27] J. Pérez-Ramírez, G. Mul, F. Kapteijn, J.A. Moulijn, J. Catal. 208 (2002) 211.
[28] G.D. Pirngruber, J. Catal. 219 (2003) 456.
[29] D.A. Bulushev, L. Kiwi-Minsker, A. Renken, J. Catal. 222 (2004) 389.
[30] J. Pérez-Ramírez, J. Catal. 227 (2004) 512.
[31] J. Pérez-Ramírez, E.V. Kondratenko, Chem. Commun. (2003) 2152.
[32] J. Pérez-Ramírez, A. Gallardo-Llamas, J. Catal. 223 (2004) 382.
[33] G.I. Panov, A.K. Uriarte, M.A. Rodkin, V.I. Sobolev, Catal. Today 41 (1998) 365.
[34] G.I. Panov, Cattech 4 (2000) 18.
[35] K.A. Dubkov, V.I. Sobolev, G.I. Panov, Kinet. Catal. 39 (1998) 79.
[36] K.A. Dubkov, N.S. Ovanesyan, A.A. Shteinman, E.V. Stakoron, G.I. Panov, J. Catal. 207 (2002) 341.
[37] J. Nováková, M. Schwarze, Z. Tvarůzková, Z. Sobalík, Catal. Lett. 98 (2004) 123.
[38] J. Jia, B. Wen, W.M.H. Sachtler, J. Catal. 210 (2002) 453.
[39] J. Nováková, M. Lhotka, Z. Tvarůzková, Z. Sobalík, Catal. Lett. 83 (2002) 215.
[40] J. Leglise, J.O. Petunchi, W.K. Hall, J. Catal. 86 (1984) 392.
[41] J. Valyon, W.S. Millman, W.K. Hall, Catal. Lett. 24 (1994) 215.
[42] J. Nováková, Z. Sobalík, Catal. Lett. 89 (2003) 243.
[43] M.N. Debbagh Boutarbouch, J.M. García Cortés, M. Soussi El Begrani, C. Salinas Martínez de Lecea, J. Pérez-Ramírez, Appl. Catal. B 54 (2004) 115.